Available online at www.sciencedirect.com
SCIENCE DIRECT®
Biochimica et Biophysica Acta 1617 (2003) 10–21
BIOCHIMICA ET BIOPHYSICA ACTA
BBA
www.bba-direct.com

Preparation and electrochemical behavior of gramicidin-bipolar lipid monolayer membranes supported on gold electrodes

J.-M. Kim[a], A. Patwardhan[b], A. Bott[c], D.H. Thompson[b,*]

[a] *Janus Biosystems, 3000 Kent Avenue, West Lafayette, IN 47906, USA*
[b] *Department of Chemistry, Purdue University, West Lafayette, IN 47907-1393, USA*
[c] *BioAnalytical Systems, Inc., 2701 Kent Avenue, West Lafayette, IN 47906, USA*

Received 6 January 2003; received in revised form 5 August 2003; accepted 28 August 2003

Dedicated to the memory of Michael J. Weaver, deceased March 21, 2002

Abstract

Gramicidin-containing synthetic bolalipid membranes comprised of 2,2′-di-*O*-decyl-3,3′-*O*-1″,20″-eicosanyl-bis-*rac*-glycero-1,1′-diphosphocholine (C20BAS) have been synthesized and supported on gold electrodes. Supported membranes were prepared by first depositing a partial bolalipid layer on the electrode using a thioctic acid-modified bolalipid (1′-*O*-ω-thioctamidetetraethylene glycol-2,2′-di-*O*-decyl-3,3′-di-*O*-1″,20″-eicosanyl-bis-*rac*-glycero-1-phosphate, SSC20BAS) as an anchoring group, followed by a vesicle fusion step using either pure C20BAS or gramicidin-containing C20BAS (C20BAS-GA) vesicles. The latter configuration was designed to immobilize single, continuously-on channels of gramicidin in the C20BAS membrane. Vesicle deposition to form supported bolalipid monolayer membranes was monitored by impedance spectroscopy and cyclic voltammetry. Impedances were observed to increase with vesicle deposition time. Pretreatment of the impedance electrode with SSC20BAS accelerated the supported monolayer membrane deposition rate. Impedances decreased in a gramicidin concentration-dependent manner when gramicidin was incorporated into the C20BAS membrane. These supported bolalipid membranes are also surprisingly inert to organic solvent exposure (CH_3CH_2OH;CH_2Cl_2), suggesting that they may serve as robust host matrices for integral membrane protein-based sensors.

Keywords: Bolalipid; Monolayer membrane; Impedance spectroscopy; Cyclic voltammetry; Supported membrane; Gramicidin

1. Introduction

Developmental efforts in membrane-based biosensors have largely focused on naturally occurring lipid membrane materials such as diacylglycerophospholipids, since they can provide a natural matrix for the incorporation of membrane proteins as functional elements for analyte recognition and/or signal transduction. Initial studies in this area focused on the preparation and physical properties of planar supported membranes on a variety of inorganic supports [1–7]. It is now possible to form unilamellar fluid supported bilayer membranes in geometrically well-defined shapes that are chemisorbed onto hydrophilic surfaces via a thin layer (~10 Å) of trapped water [8–11]. Immobilization of integral membrane proteins within these supported membranes has been accomplished by absorbing reconstituted proteoliposomes on planar substrates using a surface-vesicle fusion technique [12,13]. Supported bilayer membranes have many possible configurations, including solid supported bilayer lipid membranes [14], polymerized bilayers [15], chemisorbed bilayers [8–13], electrostatically absorbed bilayers [6,16], and tethered bilayers (t-BLM) that use either thiol-gold [7,17] or siloxy [18] bonds to couple the supported membrane to the solid substrate. The stability of t-BLM, relative to conventional black lipid membranes, makes them promising candidates for construction of membrane-based biosensors.

Vogel and co-workers have reported several systems, including thiol supported t-BLM, for investigating (1) the interactions of cholera toxin gangliosides [19], (2) the gating properties of the porin OmpF using surface plasmon resonance and impedance spectroscopy techniques [20], and (3)

* Corresponding author. Tel.: +1-765-494-0386; fax: +1-765-496-2592.
E-mail address: davethom@purdue.edu (D.H. Thompson).

0005-2736/$ - see front matter © 2003 Elsevier B.V. All rights reserved.
doi:10.1016/j.bbamem.2003.08.011

SSC20BAS (Anchor Lipid)

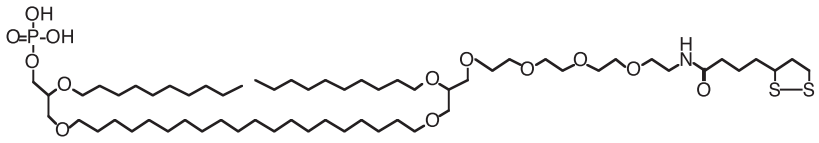

C20BAS

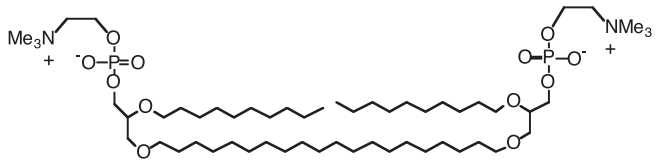

Gramicidin A (GA)

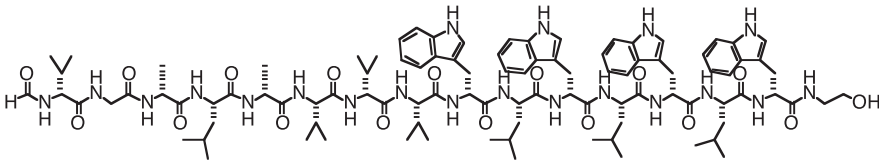

Scheme 1.

the action of the G protein-coupled receptor, bacteriorhodopsin, upon illumination in the presence of its complementary G proteins in solution [21]. Mrksich et al. [22] have demonstrated biospecific adsorption of carbonic anhydrase to a benzenesulfonamide group that was coupled to an alkanethiol anchoring group. Specific and reversible attachment of a fused β-galactosidase/choline-receptor protein using a thiol-gold tether was also demonstrated by Madoz et al. [23]. Cornell and co-workers [7,10,11] have engineered an elegant biosensor that uses chemically modified dimeric gramicidin (GA) ion channels as a switch. A mixture of bolaamphiphiles derived from thermophilic archaebacteria, and their thiol-modified analogs that linked a distal F_{ab} fragment via a polyethylene glycol spacer, were used to construct a t-BLM sensor. This sensor contains two types of gramicidin channels, one that is tethered to an F_{ab} fragment at the bulk solution-membrane interface and the other that is fixed to the electrode interface via a thiol linkage. The operating principle of this biosensor is the gating of dimeric gramicidin channels by modulating the transmembrane ion current between two states: open channels that support high ion currents when no antigen is bound, and closed channels that produce low ion currents when antigen binding causes the anchored bolalipid and gramicidin-Fab fragments to diffuse apart. Wiess-Wichert et al. [24] have reported a different biosensor design based on gramicidin channels and bolaamphiphiles that employs lipid mixtures and bisgramicidin immobilized on gold. Motesharei and Ghadiri [25] have incorporated self-assembling β-peptide nanotubes within supported membranes on gold to study their ion conduction properties. Recently, Zhao and Tamm [26] have reported a t-BLM system for the study of

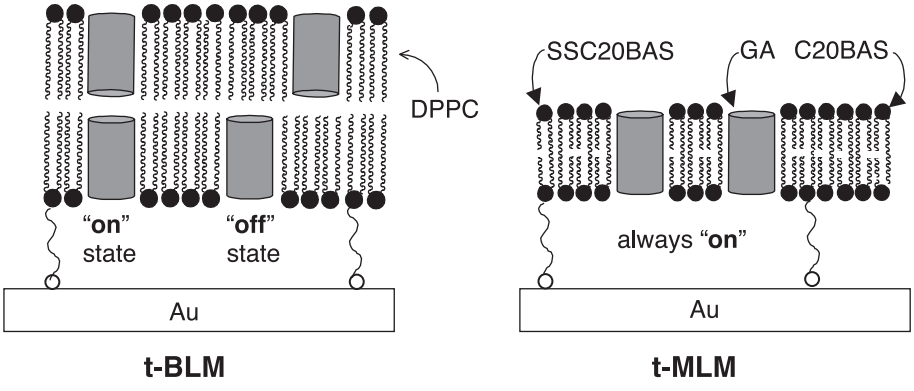

Scheme 2.

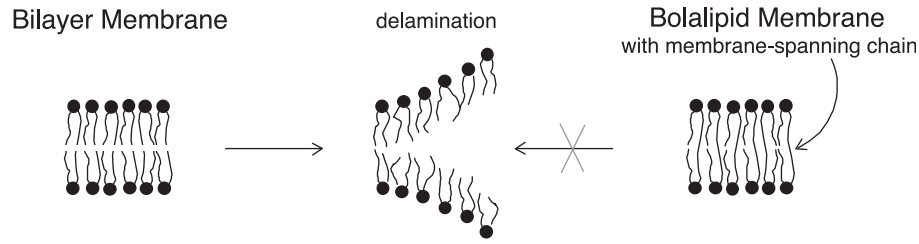

Scheme 3.

the membrane-bound synaptic fusion proteins v- and t-SNARE using FTIR and fluorescence techniques.

Major challenges remain in the design of membrane-based biosensors. Issues that limit the performance of these devices include the need for better control over molecular orientation, lateral organization, improved sensitivity, enhanced stability, and the adaptation of supported membrane sensors to diverse applications such as multianalyte detection for high throughput analysis. In this study, we sought to enhance the sensitivity and stability of gramicidin-containing t-BLM. Our strategy is based on the use of gramicidin monomers in ultrathin bolalipid monolayer membranes. Previous work from this laboratory has shown that the tetraether bolalipid, 2,2′-di-*O*-decyl-3,3′-di-*O*-eicosanyl-bis-*rac*-glycero-1,1′-diphosphocholine (C20BAS, Scheme 1), forms monolayer membrane vesicles with a ~2.0-nm-thick hydrophobic layer that is impermeable to low molecular weight solutes, while retaining the ability to passively conduct Na^+ [27–30]. Since the thickness of the bolalipid membrane [31,32] is similar to the monomeric length of the GA channel (1.5 nm) [33], we anticipated that the sensitivity of GA-containing C20BAS membranes (C20BAS-GA) supported on gold electrodes (i.e. tethered monolayer membranes, t-MLM) would increase due to the "always on" configuration of the channel relative to the flickering conductive states formed by dimeric GA channels in conventional bilayer membranes (Scheme 2). We also expected that the supported monolayer membranes would be much more stable than the bilayer structures on gold surfaces, since mechanical failure pathways due to monolayer-monolayer delamination are eliminated if the bolalipids adopt a transmembrane configuration as previously reported [34] (Scheme 3). Iida et al. [35] have recently reported findings consistent with this, wherein immobilized Bchl-polypeptides in archaebacterial tetraether lipids on gold electrodes showed higher stability than other lipids under high temperature and acidic conditions. Studies with polymerized supported bilayers [36,37] also show that the greatest mechanical stability results when inter-monolayer cross-linking occurs, providing additional support for this concept. To determine whether enhanced stability occurs for C20BAS supported membranes, we investigated the effects of bolalipid deposition, GA incorporation, and solvent exposure on the impedance and cyclic voltammetric behavior of C20BAS t-MLM on gold electrodes.

2. Experimental methods

All chemicals were purchased from Aldrich Chemical Co., except as noted. 2-Chloro-2-oxo-1,3,2-dioxaphospholane and gramicidin were obtained from Fluka and Sigma, respectively. 1,3-Diaminopropane, potassium *tert*-butoxide, 2-octyn-1-ol and 2-decyn-1-ol were purchased from Lancaster. All solvents were reagent grade and were distilled under argon before use: tetrahydrofuran (THF) from benzophenone ketyl, dichloromethane (CH_2Cl_2) from P_2O_5, and triethylamine (Et_3N) from calcium hydride (CaH_2). Toluene was used as received. All reactions were performed under inert gas (Ar or N_2) unless otherwise state. NMR spectra were recorded using ^1H or ^{13}C solvent peaks as internal reference (e.g., $CDCl_3$: 7.240 and 77.00 ppm for ^1H and ^{13}C, respectively). Column chromatography was typically performed on 60–200 mesh silica gel using high-grade solvents as eluent. Thin layer chromatography was performed using Baker-flex IB-F plates (J. T. Baker) and visualized using two or more of the following methods: UV, I_2 adsorption, $KMnO_4$/heat, and molybdic acid/heat.

2.1. Synthesis

The preparation of C20BAS has been previously described [27]. An advanced intermediate in the synthesis of C20BAS [2,2′-di-*O*-decyl-3,3′-*O*-1″,20″-eicosanyl-bis-*rac*-glycerol (**I**)] was used to prepare the anchor lipid, SSC20BAS, as shown in Fig. 1.

2.2. 2-{2-[2-(2-axido-ethoxy)-ethoxy]-ethoxy}-ethyl methanesulfonate (II)

To tetraethylene glycol (10.0 g, 51.48 mmol) was added Et_3N (8.1 g, 80 mmol) in CH_2Cl_2 at 0 °C. Methanesulfonyl chloride (8.8 g, 77.2 mmol) was then added to the flask and the reaction stirred at 25 °C for 1 day before quenching with H_2O (100 ml). The aqueous phase was extracted with EtOAc (3 × 25 ml) and the organic phases combined, dried over anhydrous $MgSO_4$, filtered, the solvent removed on a rotary evaporator, and the residue dried under vacuum to give 11.6 g (64.87% yield) of the corresponding dimesylate. ^1H (300 MHz, $CDCl_3$): 3.05 (s, 6H, CH_3); 3.6 (s, 8H, $((CH_2CH_2)_2O)$; 3.75 (m, 4H, β-CH_2O); 4.35 (m, 4H, CH_2O).

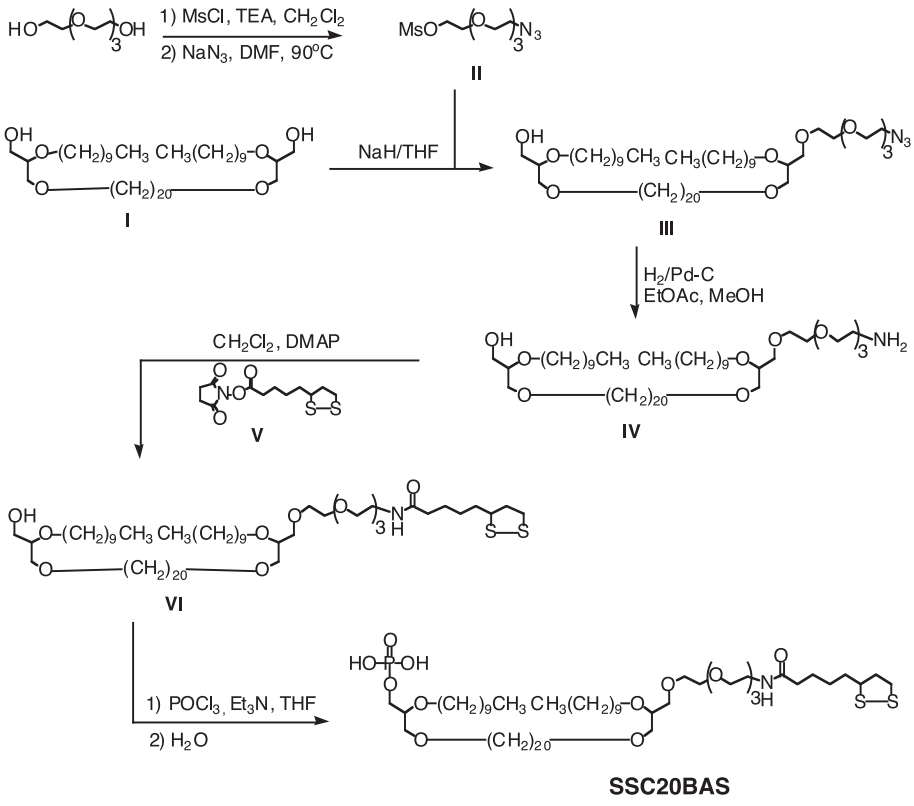

Fig. 1. Synthesis scheme for SSC20BAS.

The dimesylate from above (11.6 g, 33.35 mmol) was combined with NaN_3 (2.7 g, 33.56 mmol) in DMF (30 ml) and heated overnight at 90 °C. The reaction was then cooled to 25 °C and quenched with H_2O (100 ml). The aqueous phase was extracted with EtOAc (3 × 50 ml), the organic phases combined, dried over anhydrous $MgSO_4$, filtered, and the solvent concentrated on a rotary evaporator. The crude oil was purified via column chromatography using 1:1 hexane/EtOAc as eluent. Fractions at $R_f = 0.3$ were combined, the solvent removed using a rotary evaporator, and the residue dried under vacuum to give 2.3 g (23.4% yield) of **II**. ^1H (300 MHz, $CDCl_3$): 3.05 (s, 3H, CH_3); 3.4 (m, 2H, CH_2N_3); 3.65 (s, 10H, $(CH_2CH_2)_2OCH_2$); 3.8 (m, 2H, β-CH_2O); 4.4 (m, 2H, CH_2O).

2.3. 1-O-(ω-Azido-tetraethylene glycol)-2,2′-di-O-decyl-3,3′-di-O-1″,20″-eicosanylbis-rac-glycerol (III)

To a flask under nitrogen was added NaH (33.0 mg, 1.35 mmol) and **I** (1.0 g, 1.345 mmol), followed by 10-ml THF. Compound **II** (200 mg, 0.673 mmol in 5-ml THF) was then added and the reaction heated at reflux for 18 h before cooling to 25 °C and quenching with H_2O (50 ml). The aqueous phase was extracted with EtOAc (3 × 50 ml). The organic phase was dried over anhydrous $MgSO_4$, filtered, and evaporated to give a crude oil that was purified by column chromatography with 4:1 hexane/EtOAc as eluent. Fractions at $R_f = 0.1$ were pooled and the solvent removed under vacuum to give 0.3226 g (50.75% yield) of **III** (300 MHz, $CDCl_3$): 0.85 (t, 6H, CH_3); 1.25 (bs, 60H, CH_2); 1.65 (m, 8H, β-CH_2); 3.3-3.6 (m, 18H, CH_2O); 3.65 (m, 16H, CH_2O, CH_2N_3).

2.4. 1-O-(ω-Amino-tetraethylene glycol)-2,2′-di-O-decyl-3,3′-di-O-1″20″-eicosanyl-bis-rac-glycerol (IV)

Compound **III** (322.6 mg, 0.3415 mmol) and Pd-C catalyst (50 mg) were dissolved in 10 ml (9:1) EtOAc/MeOH in a Fischer-Porter tube and the reactor pressurized with 50 psi H_2. The reaction was stirred at 25 °C for 1 day before venting to atmosphere. The solution was filtered through a pad of Celite and the filtrate concentrated to give **IV** as an oil (0.2627 g, 83.77% yield). ^1H (300 MHz, $CDCl_3$); 0.85 (t, 6H, CH_3); 1.25 (bs, 60H, CH_2); 1.65 (m, 8H, β-CH_2); 3.3-3.6 (m, 18H, CH_2O); 3.65 (m, 16H, CH_2O); 3.95 (bs, 2H, NH_2).

2.5. 2,5-Dioxopyrrolidine-1-yl-5-[1,2]dithiolan-3-yl-pentanoate (V)

Thioctic acid (500 mg, 2.423 mmol), EDCI (700 mg, 3.64 mmol), DMAP (300 mg, 2.423 mmol), and CH_2Cl_2 (10 ml) were stirred at room temperature for 10 min prior to the addition of *N*-hydroxylsuccinimide (NHS-OH) (420 mg, 3.64 mmol). The reaction was then stirred at 25 °C for 1

day prior to quenching with H_2O (30 ml) and extraction with CH_2Cl_2 (3 × 25 ml). The organic phases were combined, filtered, evaporated, and the crude solid purified via column chromatography using EtOAc as eluent. Fractions at $R_f = 0.08$ were combined and the solvent removed to give **V** (0.4816 g, 65.50% yield). ^1H (300 MHz, $CDCl_3$): 1.4-1.83 (m, 8H, CH_2); 1.95 (p, ^1H, CH); 2.42 (p, ^1H, CH); 2.83 (s, 4H, CH_2); 3.16 (m, 2H, CH_2); 3.58 (m, ^1H, CH).

2.6. 1-O-(ω-Thioctamidetetraethylene glycol)-2,2′-di-O-decyl-3,3′-di-O-1″,20″-eicosanyl-bis-rac-glycerol (VI)

Compounds **IV** (262.7 mg, 0.286 mmol) and **V** (86.78 mg, 0.286 mmol) and Et_3N (29.0 mg, 0.286 mmol) were stirred in 5-ml CH_2Cl_2 at 25 °C for 1 day prior to quenching with H_2O (5 ml). The aqueous phase was extracted with Et_2O (3 × 25 ml), the organic phases combined, dried, filtered, and evaporated to give an oil that was purified by column chromatography (1:1 hexane/EtOAc eluent). $R_f = 0.15$ fractions were pooled and the solvent removed to give 0.1222 g (38.16% yield) of **VI**. ^1H (200 MHz, $CDCl_3$); 0.85 (t, 6H, CH_3); 1.25 (bs, 60H, CH_2); 1.5-1.7 (m, 14H, CH_2): 2.2-2.8 (m, 7H, CH_2, CH); 3.3-3.7 (m, 34H, CH_2O); 6.45 (bs, ^1H, NH).

2.7. 1′-O-(ω-Thioctamidetetraethylene glycol)-2,2′-di-O-decyl-3,3′-di-O-1″,20″-eicosanyl-bis-rac-glycero-1-phosphate (SSC20BAS)

Compound **VI** (122.2 mg, 1.104 mmol), Et_3N (300 mg, 3.0 mmol), and THF (5 ml) were added to a flask under N_2 at 5 °C. $POCl_3$ (330mg, 2.145 mmol) dissolved in 3-ml THF was then added over the course of 15 min. The reaction mixture was stirred at 25 °C for 18 h, quenched with H_2O (5 ml), and the mixture washed with 50 ml of acidic water (pH 1) and $CHCl_3$ (3 × 50 ml). The organic phases were combined, dried, filtered, and evaporated to give 0.120 g (92% yield) of solid **SSC20BAS**. ^1H (300 MHz, $CDCl_3$): 0.85 (t, 6H, CH_3); 1.25 (bs, 60H, CH_2); 1.5–1.7 (m, 14H, CH_2); 2.2–2.8 (m, 7H, CH_2, CH); 3.2 (t, 2H, $CH_2OPO_2H_2$); 3.3–3.7 (m, 32H, CH_2O). ^{13}C (75 MHz, $CDCl_3$): 13.974, 22.533, 25.491, 25.945, 25.992, 26.058, 29.190, 29.363, 29.457, 29.504, 29.550, 29.958, 31.760, 46.262, 70.450, 70.644, 70.704, 71.285, 71.519, 77.741. ^{31}P (80.9 MHz, $CDCl_3$): −0.245.

2.8. Preparation of t-MLM

Gold impedance electrodes (area = 20 mm^2) were polished using 1-μm diamond powder in methanol, rinsed with methanol and 18 MΩ water (Millipore MilliQ), and then used immediately. SSC20BAS anchor lipid was deposited by immersing the electrodes in ethanolic solutions containing 2 mM SSC20BAS for various times, followed by vigorous rinsing with an ethanol stream. t-MLM formation was completed by immersing the partially SSC20BAS-coated electrode for 24 h into 2 mM sonicated small unilamellar vesicle (SUV) solutions comprised of either pure C20BAS or C20BAS-GA of varying GA content. Vesicle solutions were prepared by dissolving the lipid mixture in $CHCl_3$, drying overnight under a 50-μ vacuum to give a thin lipid film, hydrating with pure water, and sonicating (50 W for 5 min) at 5 °C using a probe-type sonicator (Branson W-350) to give slightly turbid SUV dispersions. GA-containing C20BAS monolayer membrane vesicles showed characteristic β-helical circular dichroism behavior [32] as described for micellar [38] and bilayer membrane dispersions [39]. All supported membrane electrodes were maintained in a fully hydrated state.

2.9. Electrochemical measurements

2.9.1. Impedance spectroscopy

Impedance and phase angle measurements were made using an IM-6 electrochemical impedance spectrometer (Bioanalytical Systems BAS, Inc.) in a three-electrode configuration with the surface modified electrode serving as the working electrode. The impedance cell contained 100 mM NaCl as electrolyte. The impedance and phase angle spectra were acquired at 23 °C in the 0.1–100 kHz frequency range.

2.9.2. Cyclic voltammetry

Cyclic voltammograms were recorded using an EG&G Princeton Applied Research Model 263A instrument at a 50 mV/s scan rate. Electrolytes for CV experiments were prepared from 0.1 M KCl and 1 mM $K_3Fe(CN)_6$ (double distilled, CFS Chemicals) using ultrapure water. A platinum wire was used as the reference electrode and the membrane-deposited gold surface as both the working and counter electrodes. Potentials are reported versus SCE. N_2 gas was continuously purged through the electrochemical cell during the voltametric measurements.

3. Results and discussion

3.1. Synthesis of SSC20BAS

Since relatively few synthetic methods exist for unsymmetrically substituted bolalipids [10,40], a simple and direct synthetic method was sought for the preparation of SSC20BAS to promote t-MLM formation. The route developed is based on our previously reported symmetrical bolalipid synthesis, except that stoichiometric control was used to selectively modify the opposing headgroups with phosphate and disulfide-terminated oligo(oxyethylene) substituents (Fig. 1). The key steps in this sequence are the thioctic acid NHS ester coupling (i.e. **IV** → **VI**) and phosphorylation (i.e. **VI** → **SSC20BAS**) reactions. A range of conditions was explored in these transformations, however,

harsher conditions were found to destroy the thioctic acid moiety.

3.2. Deposition of C20BAS t-MLM onto Au

Richter and Brisson [41] have recently used atomic force microscopy to show that supported bilayer membranes can be formed on rough substrates by fusing sonicated SUV onto various solid supports. We employed cyclic voltammetry as a probe for the conditions leading to supported membrane formation on gold electrodes when SUV comprised of monolayer membrane forming lipids such as C20BAS are used. Immersion of bare gold electrodes into ethanolic SSC20BAS solutions at 25 °C for various times produced surfaces with voltammetric responses that displayed decreasing electrochemical reversibility of $Fe(CN)_6^{3-}$ as SSC20BAS exposure time increased (Fig. 2). These data suggest that longer immersion times produced adsorbed SSC20BAS films that were increasingly capable of blocking $Fe(CN)_6^{3-}/Fe(CN)_6^{4-}$ access to the gold electrode surface. When exposure times exceeded 3 h, the SSC20BAS anchor lipid films passivated the surface toward $Fe(CN)_6^{4-}/Fe(CN)_6^{3-}$ redox processes, suggesting that essentially continuous lipid layers were deposited. Time-dependent impedance and phase angle properties of SS20BAS-deposited gold electrodes showed similar effects—impedances were found to increase with increasing deposition time (Fig. 3). Based on these data, subsequent experiments utilized 60-min im-

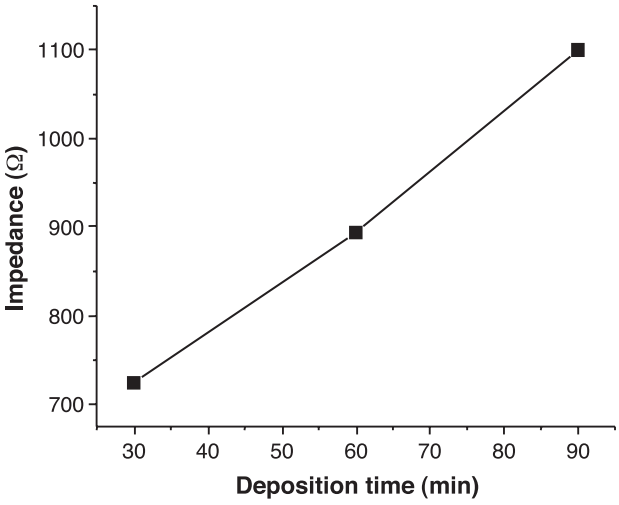

Fig. 3. Impedance changes at 1×10^5 Hz as a function of deposition time for SSC20BAS (2 mM in CH_3CH_2OH) on gold electrodes.

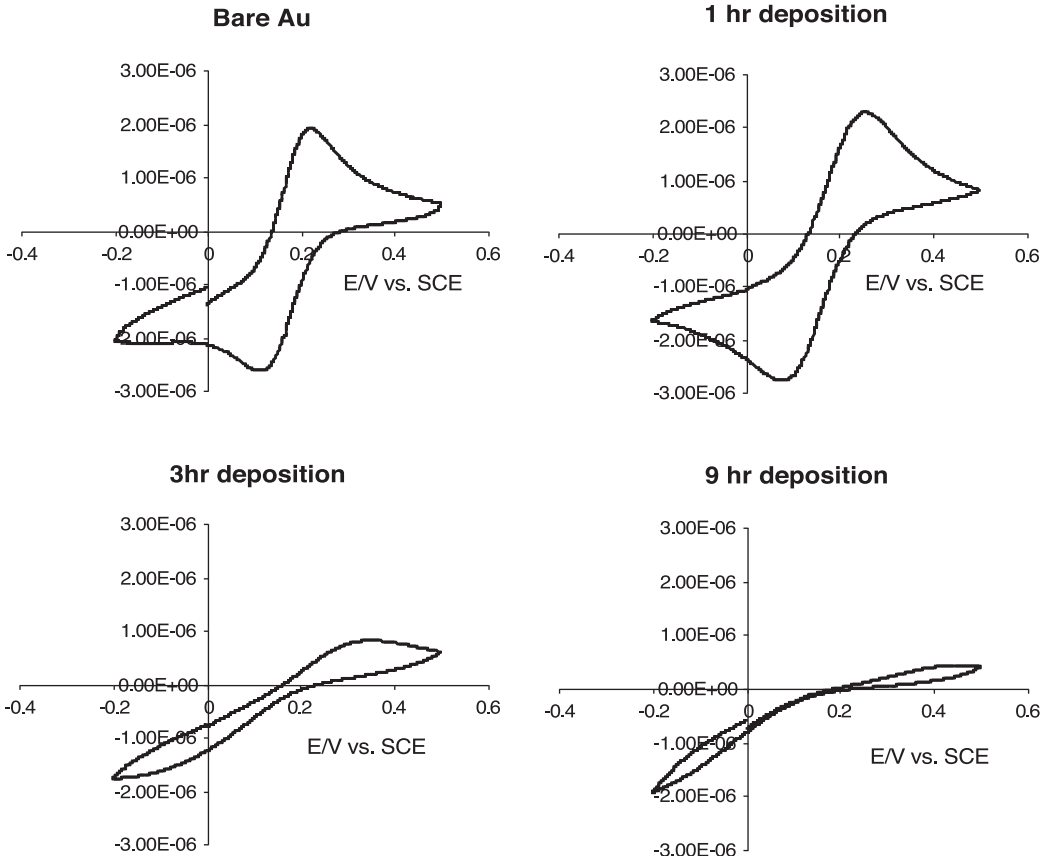

Fig. 2. Cyclic voltammograms of Au electrodes treated with SSC20BAS for varying time periods. The electrodes were coated by immersion into 2 mM SSC20BAS in CH_3CH_2OH for 0, 1, 3, and 9 h, air-dried, and analyzed using anaerobic solutions of 1 mM $K_3Fe(CN)_6^{3-}$ in 0.1 M $HClO_4$ (50 mV/s, Pt ref. vs. SCE).

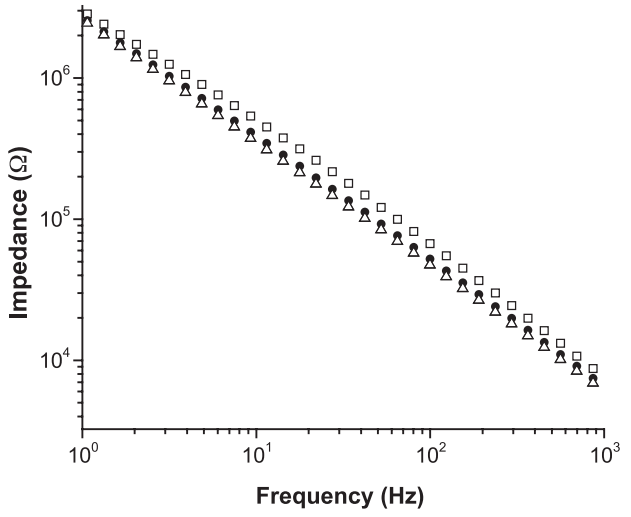

Fig. 4. Impedance spectra of C20BAS t-MLM on gold electrodes treated with sonicated SUV of different GA/C20BAS molar ratios (25 °C, pH 7.4, 100 mM NaCl). (□) 1:500 GA/C20BAS; (●) 1:100 GA/C20BAS; (△) 1:50 GA/C20BAS.

mersion times for SSC20BAS solutions prior to fusion with C20BAS or C20BAS-GA SUV to deposit t-MLM films.

3.3. Effect of increasing gramicidin/lipid ratios

The effect of gramicidin surface density on supported membrane impedance was determined using electrodes that had been coated with t-MLM by pretreatment with SSC20BAS prior to immersion for 24 h into sonicated C20BAS-GA vesicles containing varying amounts of gramicidin.[1]

Impedance measurements with these C20BAS-GA t-MLM electrodes showed impedance decreases with increasing GA concentration over the entire $1-10^3$ Hz range examined (Fig. 4), indicating that a functional ion channel form of gramicidin is incorporated within the C20BAS monolayer membrane. Relatively small changes in impedance were observed as the gramicidin/bolalipid ratio was increased, suggesting that either (1) the t-MLM has a maximum gramicidin capacity near the 1:100 GA/C20BAS ratio, (2) the ion flux through the channel is sufficiently fast that increased surface densities of gramicidin channels has little influence on impedance behavior, or that (3) gramicidin has little influence on the electrical properties of the t-MLM. The second explanation is most consistent with our ^{23}Na NMR ion flux and single channel measurements for gramicidin-containing C20BAS vesicles [30]. It is also consistent with the observations of Krishna et al. [11] who have shown that the conductance of gramicidin in t-BLM systems varies monotonically with GA concentrations. Their work also shows that the apparent channel conductivity is an order of magnitude lower than GA in conventional bilayer membranes, suggesting that the entrapped aqueous reservoir can have a significant effect on the overall conductivity of the membrane. The data in Fig. 4 suggest that the C20BAS-GA t-MLM impedance may also be affected by the reservoir properties; however, additional studies are needed to probe this effect.

3.4. Stepwise construction of t-MLM films

The effects of gramicidin loading on t-MLM electrode impedance were further investigated in a series of sequential deposition experiments (Fig. 5). Adsorption of SSC20BAS onto Au electrodes for 1 h produced significant increases in impedance as expected due to partial surface coverage (Fig. 3). Immersion of these pretreated electrodes into bolalipid vesicle solutions, where gramicidin was either absent or present (i.e. C20BAS and C20BAS-GA vesicles, respectively), produced t-MLM coated electrodes that had substantially different impedance characteristics in $10^{-1}-10^2$ Hz frequency range. As the data in Fig. 5 show, immersion of SSC20BAS-treated electrodes into 2 mM C20BAS membrane solutions for 24 h further increased the t-MLM impedance. We attribute this observation to the formation of a continuous, impermeable C20BAS membrane due to SSC20BAS-mediated vesicle adsorption and fusion of neighboring tethered C20BAS vesicles to form a high impedance t-MLM. When the SSC20BAS electrodes were immersed in 1:100 GA/C20BAS membrane solutions for 24 h, however, the observed impedances were much lower—approaching that of bare gold—than for either the SSC20BAS or SSC20BAS–C20BAS t-MLM coatings.

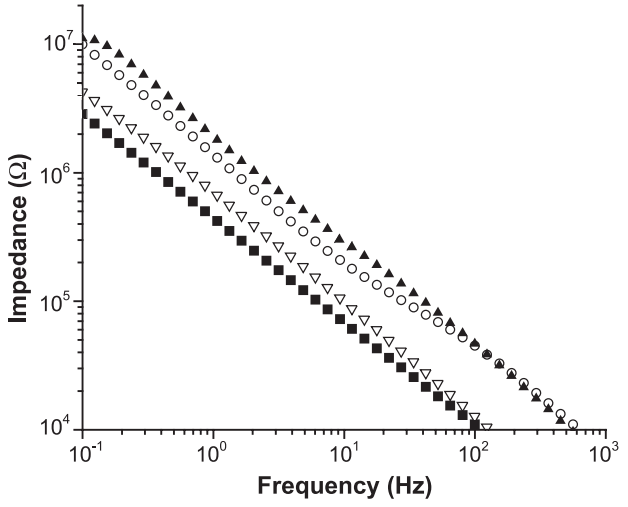

Fig. 5. Impedance spectra of the C20BAS-GA t-MLM deposition process (25 °C, pH 7.4, 100 mM NaCl). (■) Bare Au; (○) SSC20BAS; (▲) SSC20BAS–C20BAS; (△) SSC20BAS-C20BAS-GA.

[1] The nominal gramicidin/bolalipid molar ratios in our sonicated SUV preparations ranged from 1:500 to 1:50 at a 2 mM total lipid concentration. These concentrations were verified by phosphate and gramicidin analyses at high GA/C20BAS ratios. GA analysis sensitivity did not enable detection at lower ratios. GA/C20BAS ratios on the electrode surface are assumed to be the same as the nominal SUV ratios.

Similar trends were observed for phase angle measurements (Fig. 6) in the $1-10^3$ Hz frequency range for the data shown in Fig. 5. Equivalent circuit analysis shows that the typical series resistance-capacitance behavior of gold electrodes becomes more complex as the membrane film assembles on the electrode surface. Sequential deposition of SSC20BAS and C20BAS produces surfaces that are best described by a serial solution resistance element in parallel with two resistive-capacitive elements. Notably, the second deposition step generates surfaces having higher resistance at resistive elements 1 and 3 for SSC20BAS–C20BAS (73.7 MΩ and 101.7 kΩ) than the SSC20BAS-coated electrodes (43.9 MΩ and 42.9 kΩ), as would be expected if a continuous membrane film were deposited on the gold surface (Table 1). Inclusion of gramicidin in these t-MLM films, however, greatly simplifies their impedance spectra such that their properties are more similar to bare gold. The phase angle data, which show a maximum near 80° and significant deviation from the fit at low frequency for the SSC20BAS + C20BAS-GA membranes relative to bare gold electrodes, indicate that a t-MLM is present whose properties allow for ion migration through the film at low

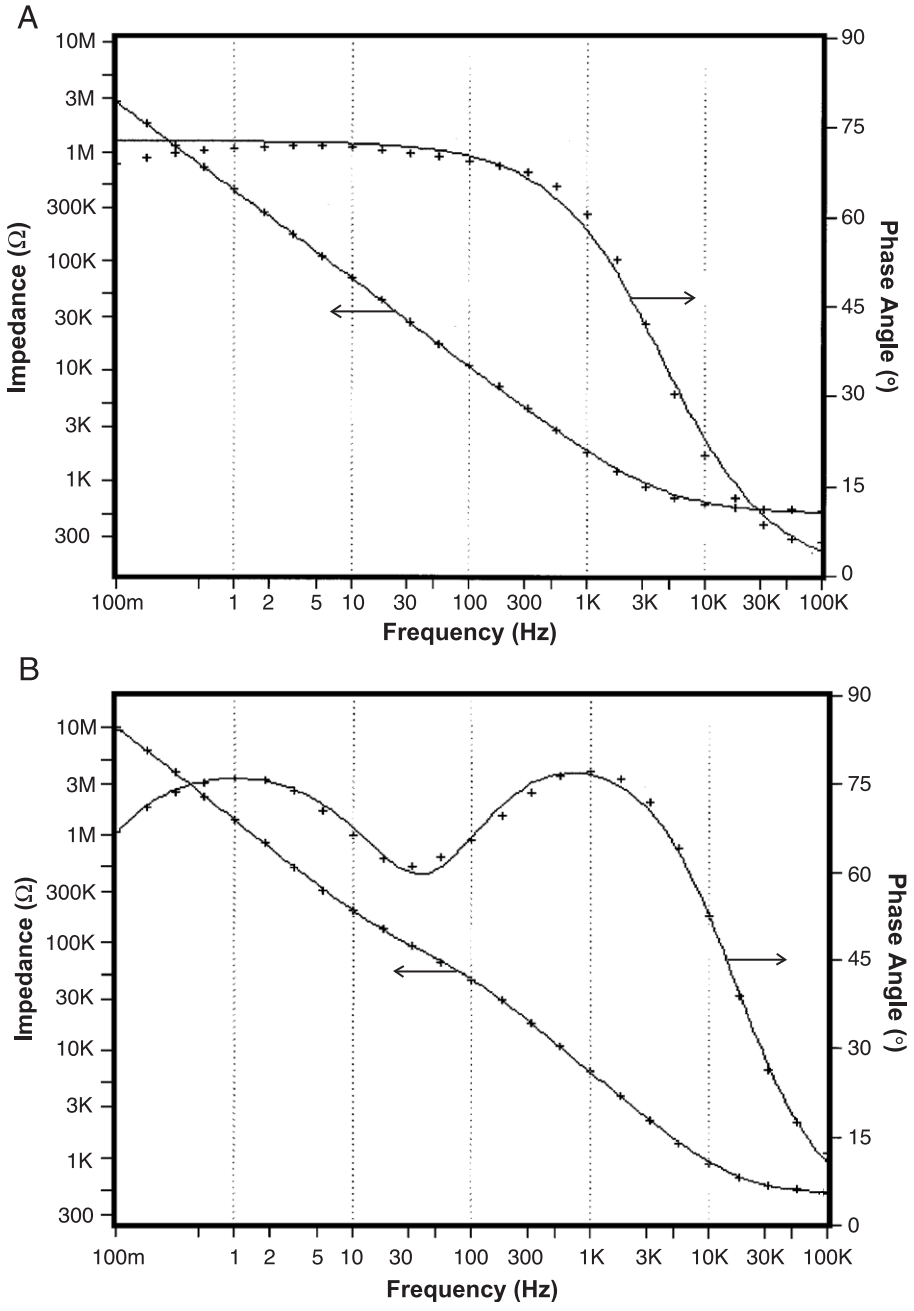

Fig. 6. Phase angle diagrams for the data shown in Fig. 5. (A) Bare gold electrode. (B) SSC20BAS on gold electrode. (C) SSC20BAS + C20BAS on gold electrode. (D) SSC20BAS + C20BAS-GA on gold electrode.

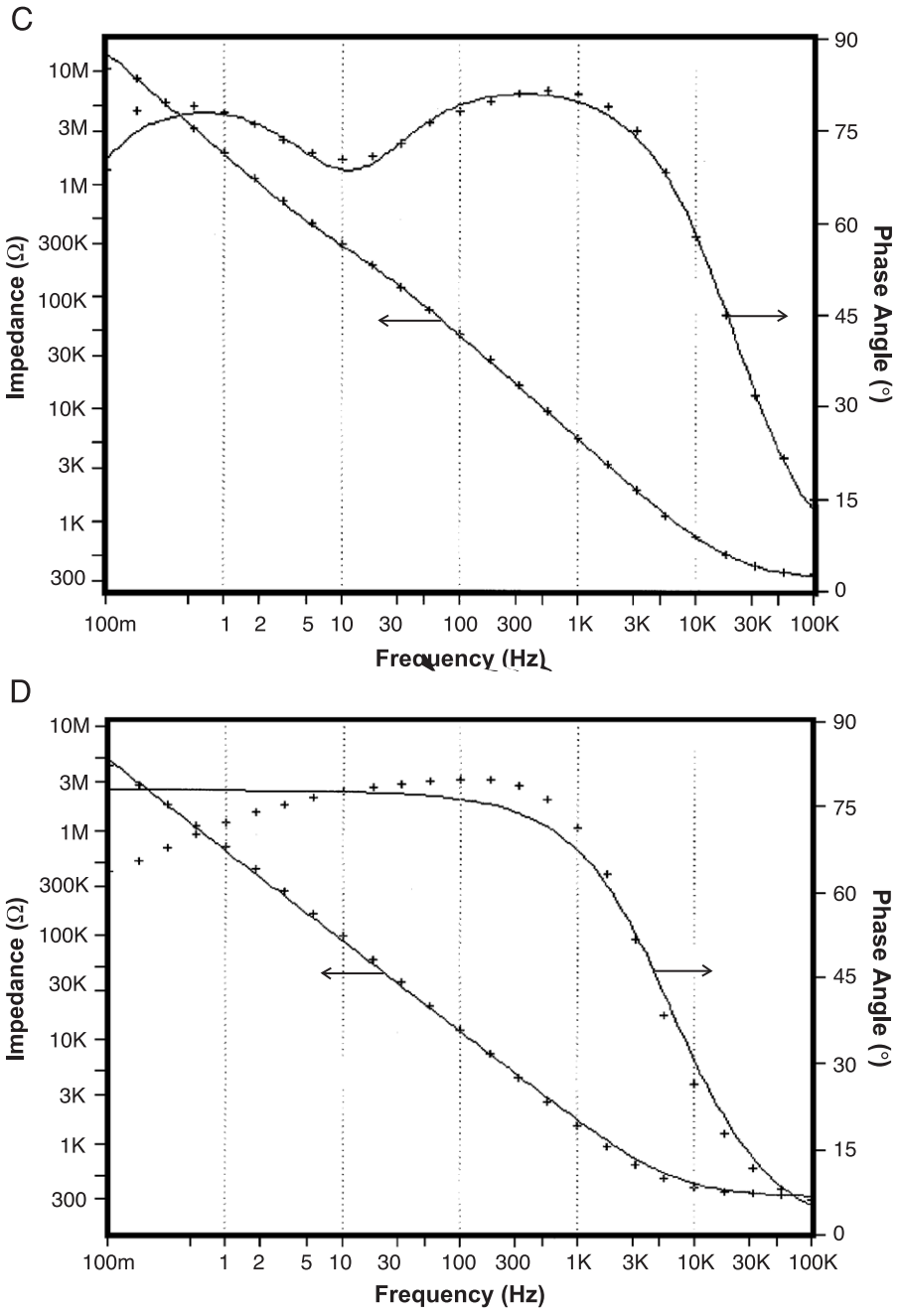

Fig. 6 (*continued*).

frequency. The cyclic voltammetry behavior of SSC20BAS-tethered C20BAS-GA coated electrodes further support this conclusion (see below). These data support the model depicted in Scheme 2 where gramicidin monomers act as monomolecular ion channels in these t-MLM constructs. We also infer from these results, and the CV response observed in Fig. 2, that the 1-h pretreatment of gold with ethanolic solutions of SSC20BAS produces films that are disordered and discontinuous (i.e. containing defect sites due to low surface coverages and/or poor bolalipid packing). These disordered surfaces become more ordered upon adsorption and fusion of bolalipid vesicle dispersions onto the partially coated electrode surface. When gramicidin-free C20BAS vesicles are used in the vesicle fusion step on the electrode surface, higher impedances are observed due to the annealing of surface defects by the more highly ordered C20BAS

Table 1

	R_1 (MΩ)	C_1 (nF)	R_2 (KΩ)	C_2 (nF)	R_3 (Ω)	C_3 (nF)
Bare Au	–	–	–	–	502	96
SSC20BAS	43.9	51.1	43	49.7	472	–
SSC20BAS + C20BAS	73.8	46.6	101.7	78.1	320	–
SSC20BAS + C20BAS-GA	–	–	–	–	323	96

membrane. When C20BAS-GA vesicles are used, the C20BAS monolayer membranes produce gold electrode surfaces with lower impedance due to the activity of monomeric gramicidin channels that are capable of passively transporting cations across the t-MLM films in response to either an applied potential or a transmembrane concentration gradient. This suggests that the membrane design can alter the ion conduction mechanism of gramicidin from a ‘‘flickering’’ dimeric channel in 40-Å-thick (bilayer) membranes to an ‘‘always on’’ monomeric channel in 20-Å-thin bolalipid membranes (Scheme 2). Similar changes in ion conduction mechanism have been reported for valinomycin in bolaform archael lipid systems [42], where a transition from a carrier-mediated process in bilayers to an ion channel mechanism in bolalipid systems is thought to occur due to the presence of an ultrathin bolalipid membrane.

3.5. Stability of supported monolayer and bilayer membranes

Gold electrodes bearing t-MLM are remarkably rugged with respect to solvent exposure compared to conventional supported bilayer membranes. Cyclic voltammetry experiments with t-BLM and t-MLM reveal that sequential washings with water and ethanol had relatively little effect on the voltammetric response of t-MLM-treated gold electrodes relative to similarly treated t-BLM electrodes (Fig. 7). Washing of t-MLM electrodes with water or ethanol produced little change in the cyclic voltammetric response of these electrodes relative to unrinsed t-MLM electrodes. Extended washing with methylene chloride, however, was able to remove enough lipid that the $Fe(CN)_6^{4-}$ oxidation wave was again observable, indicating that the passivating t-MLM lipid film that was originally present was partially removed by this treatment. These observations are in direct contrast with the behavior of DPPC-based t-BLM electrodes prepared in a similar manner. These t-BLM electrodes displayed far less resilience toward identical solvent treatments than the t-MLM surfaces; a significant increase in the $Fe(CN)_6^{4-}/Fe(CN)_6^{3-}$ cyclic voltammetric response was observed after the first rinse with ethanol. We infer from these results that C20BAS t-MLM are more robust because the membranes are more highly ordered and less prone to delamination than DPPC t-BLM (Scheme 3).

There are many possible reasons for these observed differences in stability. C20BAS is a centrosymmetric molecule, favoring the formation of planar membranes. In fact, sonicated or extruded dispersions of C20BAS tend to rapidly fuse to produce very large vesicles [28] even in the absence of sites that can catalyze vesicle aggregation and fusion. This does not prevent the formation of curved membrane surfaces, such as those that must exist on the roughened gold electrode surface, because bolalipids can accumulate U-shaped conformations in regions where the solid surface architecture dictates curvature mismatch at membrane interfaces that are proximal and distal to the electrode surface. Another possible explanation of their stability is that bolalipids prefer to adopt a membrane-spanning conformation (at least 75% of the population exists in a transmembrane orientation [34]), effectively ‘cross-linking’ the membrane and making it more mechanically rugged than conventional bilayer membranes. The importance of this effect has been clearly demonstrated by Ross et al. [37], who showed that bilayers possessing covalent inter-monolayer cross-links in the bilayer membrane are much more mechanically stable towards delamination than similar constructs possessing only intra-monolayer cross-links. Finally, the hydrophobic mismatch between the DPPC bilayer and the SSC20BAS tethering lipids can be expected to create solvent-accessible defect sites that facilitate delipidation of the gold electrode (Fig. 8). A full description of the origins of stability will require further experimentation; however, these results suggest that

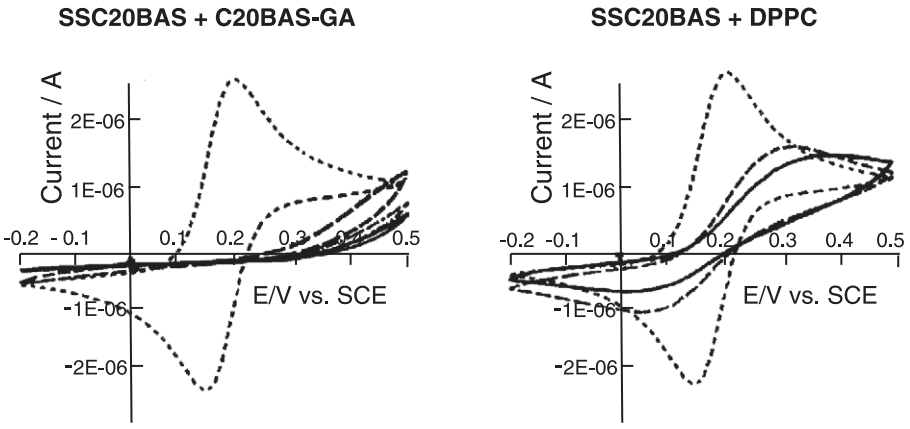

Fig. 7. Cyclic voltammograms of 1 mM $K_3Fe(CN)_6$ in 0.1 M KCl showing the stability of t-MLM relative to t-BLM (50 mV/s, Pt ref. vs. SCE). Left: (·····) SSC20BAS (30-min deposition); (—) SC20BAS + C20BAS-GA (1-day deposition), then H_2O wash; (–·–·–) EtOH wash; (– – –) CH_2Cl_2 wash. Right: (·····) SSC20BAS (30-min deposition); (—) SSC20BAS + DPPC (2-day deposition), then H_2O wash; (– – –) EtOH wash.

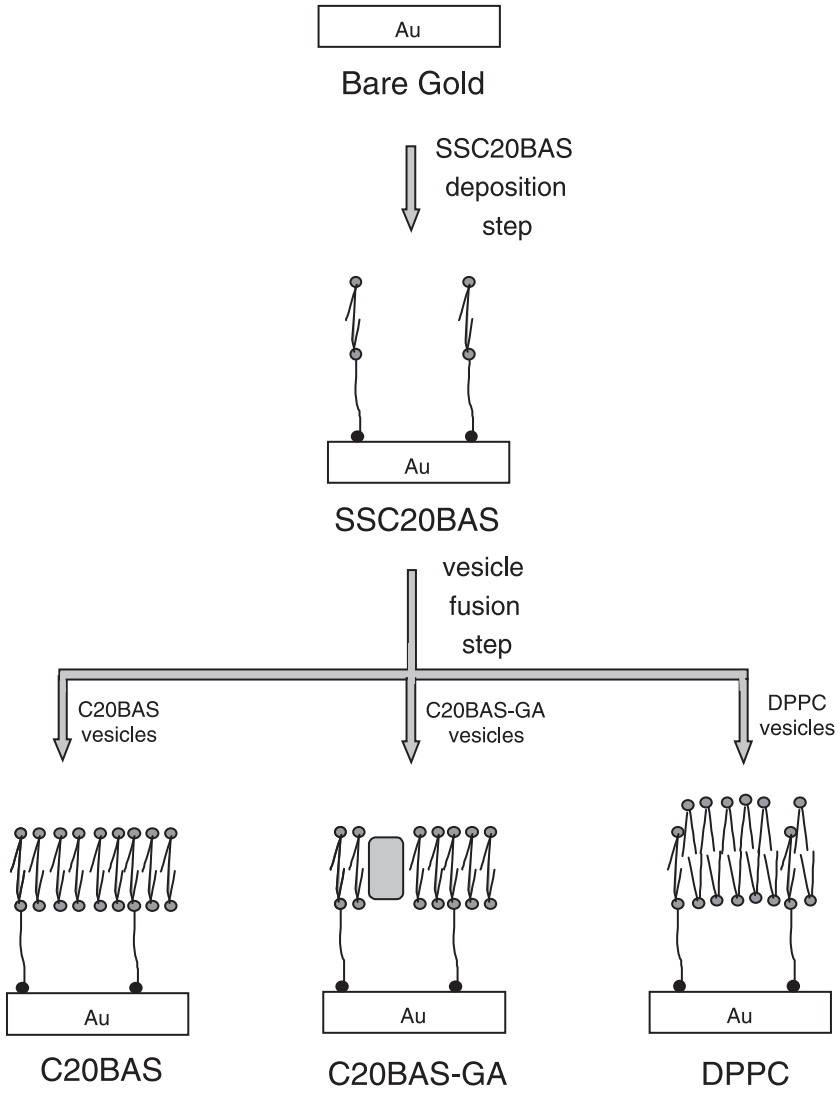

Fig. 8. Conceptual diagram of t-MLM and t-BLM preparation and organization.

bolalipid-based t-MLM may serve as a robust host matrix for integral membrane protein-based membrane sensors.

4. Conclusions

The tetraether bolalipid, C20BAS, can be co-deposited on gold with the disulfide-based anchor lipid, SSC20BAS, to form a stable t-MLM film. Incorporation of gramicidin into these t-MLM constructs produces stable membrane films with monovalent cation channels that are believed to operate in an ''always open'' conductive state. In addition, C20BAS-GA t-MLM are very stable in water and are much more resistant to organic solvent treatment than their corresponding DPPC bilayer membrane films. These results demonstrate that a stable membrane-based impedance biosensor can be constructed and that incorporation of gramicidin can produce sensor responses that are attributable to the anticipated function of the ion channel.

Acknowledgements

The authors would like to thank Mr. S. Park for assistance with the cyclic voltammetry measurements.

References

[1] L.B. Margolis, Cell-interaction with model membranes—probing, modification and simulation of cell-surface functions, Biochim. Biophys. Acta 779 (1984) 161–189.
[2] H.M. McConnell, T.H. Watts, R.M. Wies, A.A. Brian, Supported planar membranes in studies of cell–cell recognition in the immune-system, Biochim. Biophys. Acta 864 (1986) 95–106.
[3] E. Kalb, S. Frey, L.K. Tamm, Formation of supported planar bilayers by fusion of vesicles to supported phospholipid monolayers, Biochim. Biophys. Acta 1103 (1992) 307–316.
[4] N.L. Abbott, J.P. Folkers, G.M. Whitesides, Manipulation of the wettability of surfaces on the 0.1-micrometer to 1-micrometer scale through micromachining and molecular self-assembly, Science 257 (1992) 1380–1382.

[5] J.T. Groves, N. Ulman, P.S. Cremer, S. Boxer, Substrate–membrane interactions: mechanisms for imposing patterns on a fluid bilayer membrane, Langmuir 14 (1998) 3347–3350.
[6] C. Steinem, A. Janshoff, P.-W. Ulrich, M. Sieber, H.-J. Galla, Impedance analysis of supported lipid bilayer membranes: a scrutiny of different preparation techniques, Biochim. Biophys. Acta 1279 (1996) 169–180.
[7] B.A. Cornell, V.L.B. Braach-Maksvystis, L.G. King, P.D.J. Osman, B. Raguse, L. Wieczorek, R.J. Pace, A biosensor that uses ion-channel switches, Nature 387 (1997) 580–583.
[8] J.T. Groves, N. Ulman, S.G. Boxer, Micropatterning fluid lipid bilayers on solid supports, Science 275 (1997) 651–653.
[9] J. Salafsky, J.T. Groves, S.G. Boxer, Architecture and function of membrane proteins in planar supported bilayers: a study with photosynthetic reaction centers, Biochemistry 35 (1996) 14773–14781.
[10] B. Raguse, V. Braach-Maksvytis, B.A. Cornell, L.G. King, P.D.J. Osman, R.J. Pace, L. Wieczorek, Tethered lipid bilayer membranes: formation and ionic reservoir characterization, Langmuir 14 (1998) 648–659.
[11] G. Krishna, J. Schulte, B.A. Cornell, R.J. Pace, P.D. Osman, Tethered bilayer membranes containing ionic reservoirs: selectivity and conductance, Langmuir 19 (2003) 2294–2305.
[12] A.A. Brian, H.M. McConnell, Allogeneic stimulation of cytotoxic t-cells by supported planar membranes, Proc. Natl. Acad. Sci. U. S. A. 81 (1984) 6159–6163.
[13] T.H. Watts, A.A. Brian, J.W. Kappler, P. Marrack, H.M. McConnell, Antigen presentation by supported planar membranes containing affinity-purified I-AD, Proc. Natl. Acad. Sci. U. S. A. 81 (1984) 7564–7568.
[14] Q.Y. Liu, H. Ti Tien, Incorporation of bovine rod outer segments into a bilayer lipid–membrane and its transformation into a photo-excitable system, Photobiochem. Photobiophys. 4 (1982) 73–78.
[15] J.C. Conboy, S. Liu, D.F. O'Brien, S.S. Saavedra, Planar supported bilayer polymers formed from bis-diene lipids by Langmuir–Blodgett deposition and UV irradiation, Biomacromolecules 4 (2003) 841–849.
[16] C. Steinem, A. Janshoff, H.-J. Galla, M. Sieber, Impedance analysis of ion transport through gramicidin channels incorporated in solid supported lipid bilayers, Bioelectrochem. Bioenerg. 42 (1997) 213–220.
[17] H. Lang, C. Duschl, H. Vogel, A new class of thiolipids for the attachment of lipid bilayers on gold surfaces, Langmuir 10 (1994) 197–210.
[18] M.L. Wagner, L.K. Tamm, Softly supported planar bilayers for reconstitution of integral membrane proteins: a unique PEG-lipid as a cushion and tether, Biophys. J. 78 (2000) 1072.
[19] S. Terrettaz, T. Stora, C. Duschl, H. Vogel, Protein-binding to supported lipidmembranes—investigation of the cholera-toxin ganglioside interaction by simultaneous impedance spectroscopy and surface-plasmon resonance, Langmuir 9 (1993) 1361–1369.
[20] T. Stora, J.H. Lakey, H. Vogel, Ion-channel gating in transmembrane receptor proteins: functional activity in tethered lipid membranes, Angew. Chem., Int. Ed. Engl. 38 (1999) 389–392.
[21] C. Bieri, O.P. Ernst, S. Heyse, K.P. Hofmann, H. Vogel, Micropatterned immobilization of a G protein-coupled receptor and direct detection of G protein activation, Nat. Biotechnol. 17 (1999) 1105–1108.
[22] M. Mrksich, J.R. Grunwell, G.M. Whitesides, Biospecific adsorption of carbonicanhydrase to self-assembled monolayers of alkanethiolates that present benzenesulfonamide groups on gold, J. Am. Chem. Soc. 117 (1995) 12009–12010.
[23] J. Madoz, B.A. Kuznetzov, F.J. Medrano, J.L. Garcia, V.M. Fernandez, Functionalization of gold surfaces for specific and reversible attachment of a fused beta-galactosidase and choline-receptor protein, J. Am. Chem. Soc. 119 (1997) 1043–1051.
[24] C.H. Wiess-Wichert, M. Smetazko, M. Valina-Saba, T.H. Schalkhammer, A new analytical device based on gated ion channels: a peptide-channel biosensor, J. Biomol. Screen. 2 (1997) 11–18.
[25] K. Motesharei, R.M. Ghadiri, Diffusion-limited size-selective ion sensing based on SAM-supported peptide nanotubes, J. Am. Chem. Soc. 119 (1997) 11306–11312.
[26] J. Zhao, L.K. Tamm, FTIR and fluorescence studies of interactions of synaptic fusion proteins in polymer-supported bilayers, Langmuir 19 (2003) 1838–1846.
[27] A.P. Patwardhan, D.H. Thompson, Efficient synthesis of 40- and 48-membered tetraether macrocyclic bisphosphocholines, Org. Lett. 1 (1999) 241–244.
[28] C. DiMeglio, S.B. Rananavare, S. Svenson, D.H. Thompson, Phosphocholine analogs of bolaamphiphiles: phase structure and mesomorphism, Langmuir 16 (2000) 128–133.
[29] A. Patwardhan, D.H. Thompson, Novel flexible and rigid tetraether acyclic and macrocyclic bisphosphocholines: synthesis and monolayer properties, Langmuir 16 (2000) 10340–10350.
[30] A.P. Patwardhan, C. DiMeglio, R. Haynes, J.-M. Kim, D. Burden, J. Kasianowicz, D.H. Thompson, unpublished results.
[31] J.-M. Kim, D.H. Thompson, Tetraether bolaform amphiphiles as models of archaebacterial membrane lipids: synthesis, differential scanning calorimetry, and monolayer studies, Langmuir 8 (1992) 637–644.
[32] D.H. Thompson, J.-M. Kim, C. DiMeglio, Photoinduced charge transfer properties of bolaamphiphile membrane-gramicidin diad and triad composites, SPIE Proc. 1853 (1993) 142–147; see also: D.H. Thompson, J.M. Kim, Photoinduced charge transfer studies in bolaamphiphile-gramicidin-porphyrin membranes, MRS Symp. 277 1992, pp. 93–98.
[33] B.A. Wallace, K. Ravikumar, The gramicidin pore-crystal-structure of a cesium complex, Science 241 (1988) 182–187.
[34] D.H. Thompson, K. Wong, R. Humphry-Baker, J. Wheeler, J.-M. Kim, S.B. Rananavare, Tetraether bolaform amphiphiles as models of archaebacterial membrane lipids: Raman spectroscopy, ^{31}P-NMR, X-ray scattering and electron microscopy, J. Am. Chem. Soc. 114 (1992) 9035–9042.
[35] K. Iida, H. Kiriyama, A. Fukai, W.N. Konings, M. Nango, Two-dimensional self-organization of the light-harvesting polypeptides/BChl a complex into a thermostable liposomal membrane, Langmuir 17 (2001) 2821–2827.
[36] E.E. Ross, B. Bondurant, T. Spratt, J.C. Conboy, D.F. O'Brien, S.S. Saavedra, Formation of self-assembled, air-stable lipid bilayer membranes on solid supports, Langmuir 17 (2001) 2305–2307.
[37] E.E. Ross, L.J. Rozanski, T. Spratt, S. Liu, D.F. O'Brien, S.S. Saavedra, Planar supported lipid bilayer polymers formed by vesicle fusion. 1. Influence of diene monomer structure and polymerization method on film properties, Langmuir 19 (2003) 1752–1765.
[38] D.W. Urry, T.L. Trapane, K.U. Prasad, Is the gramicidin-a transmembrane channel single-stranded or double-stranded helix—a simple unequivocal determination, Science 221 (1983) 1064–1067.
[39] B.A. Wallace, W.R. Veatch, E.R. Blout, Conformation of gramicidin-a in phospholipid-vesicles—circular-dichroism studies of effects of ion binding, chemical modification, and lipid structure, Biochemistry 20 (1981) 5754–5760; see also: B.A. Wallace, Structure of gramicidin-a, Biophys. J. 49 (1986) 295–306.
[40] H.F. Heiser, B. Dobner, Novel bipolar phospholipids with different headgroups, Chem. Commun., (1996) 2025–2026.
[41] R.P. Richter, A. Brisson, Characterization of lipid bilayers and protein assemblies supported on rough surfaces by atomic force microscopy, Langmuir 19 (2003) 1632–1640.
[42] A. Gliozzi, M. Robello, L. Fittabile, A. Relini, A. Gambacorta, Valinomycin acts as a channel in ultrathin lipid membranes, Biochim. Biophys. Acta 1283 (1996) 1–3.